

OBJECT-ORIENTED MODELLING OF FLIGHT CONTROL ACTUATION SYSTEMS FOR POWER ABSORPTION ASSESSMENT

Gianpietro Di Rito, Eugenio Denti, and Roberto Galatolo
Department of Aerospace Engineering - University of Pisa

Keywords: Aircraft systems, actuators, power absorption, object-oriented modelling

Abstract

In the work, the object-oriented approach provided by the Modelica-Dymola environment is used to perform a comparison between different technologies for aircraft actuation systems in terms of power absorption characteristics. Starting from the same set of basic design, three actuators characterised by different technological solutions (servo-hydraulic, electro-hydrostatic and electro-mechanical) have been defined, and the related “object-models” have been developed and characterised in terms of dynamic performances. In parallel, the model of a basic flight control system with two ailerons, two elevators and one rudder has been created, including models for the aerodynamic hinge moments calculation and the simulation of elasticity of the actuator structural links. The models have been then used to obtain three types of actuation systems: a traditional servo-hydraulic one, a “more-electric” plant with all electro-hydrostatic actuators, and an “all-electric” system. Each system is finally tested with the same command time history by reproducing a sample flight manoeuvre, and the power absorption characteristics are analysed and discussed.

1 Introduction

The design of modern airborne systems and equipments constantly tends towards both technology innovation and integration of functions. This trend has been recently emphasized by research programs oriented to the conversion of aircraft systems to the “all-electric” solution [1, 2, 3, 4], which clearly

pointed out important issues on power management for systems [5, 6, 7]. A relevant case is that of the flight control actuators. The “all-electric” objective has rapidly driven the system engineers to evolve the actuation technology, moving from the traditional servo-hydraulic, through electro-hydrostatic, and towards electro-mechanical architectures, consequently arising new design issues related to structural interactions, thermal dissipation, energy management, and reliability [8, 9]. Furthermore, flight control actuators’ requirements become more and more extended, aiming to implement additional functions such as active vibration control, noise reduction, load alleviation.

In this context, a strong effort is required for system engineers to develop models that are capable of predicting the actuator dynamic performances, with particular attention to power absorption. The object-oriented modelling [10, 11] provides a convenient approach to this activity, since the model prototyping and the performance analysis of complex multi-physical systems can be carried out very efficiently [12].

The proposed paper focuses on the development of an object-oriented simulation platform for the study of flight control actuation systems. The platform has been entirely developed in the Modelica-Dymola environment, and provides an extensive collection of “object-models” for the simulation of modern flight actuators. To point out the potentialities of the simulation platform, a comparative analysis among different actuator technologies is performed, by evaluating the power absorption of an entire flight control

actuation system during a sample flight manoeuvre.

Starting from the same set of basic design requirements (working stroke, stall force, maximum no-load velocity, settling time of the actuator position response), three actuators characterised by different technology (servo-hydraulic, electro-hydrostatic and electro-mechanical) are defined, and the related “object-models” are developed and characterised in terms of dynamic performances. In parallel, the model of a basic flight control system composed of two ailerons, two elevators and one rudder is created, including models for the aerodynamic hinge moments calculation [13, 14]. The actuator models are then used to obtain three types of actuation systems: a traditional servo-hydraulic one, a “more-electric” system with all electro-hydrostatic actuators, and an “all-electric” plant. Each system is finally tested with the same command time history, and the power absorption characteristics are analysed and discussed.

The paper is organised into three sections: the first one is dedicated to the description of the three actuator models and to their performance characterisation, the second section is related to the model of the entire aircraft actuation system, and the final part to the power absorption assessment for the three different solutions.

2 Actuator models

This section deals with the architectural definition, the preliminary sizing and the object-oriented modelling of the three actuators in the Modelica-Dymola environment.

The actuator functional parameters have been defined starting from the basic design requirements reported in Table 1, which can be considered representative for the primary flight controls of a light military jet trainer.

Equivalent load mass	50 kg
Stiffness of the actuator link to aircraft structure	20 kN/mm
Stiffness of the actuator link to control surface	8 kN/mm
Working stroke	± 50 mm
Maximum no-load velocity	150 mm/s
Stall force	30 kN
Position response bandwidth	> 4 Hz
Position response steady-state error	$< 0.1\%$

Table 1. Basic requirements for the actuator sizing.

2.1 Servo-hydraulic actuator

A typical solution for a servo-hydraulic flight control actuation is schematically depicted in Fig. 1. The aerodynamic surface deflection is obtained by a hydraulic cylinder with fixed case and movable piston. The hydraulic power coming from a centralised pressure-controlled plant is regulated by an integrated control unit, basically composed of a proportional four-way servovalve and a bypass/damping valve system, which can be activated both hydraulically and electrically in case of failures.

The position of the servo-hydraulic actuator (SHA) is closed-loop controlled by a dedicated actuator electronic unit, which can be located in the flight control computers or integrated in the actuator assembly.

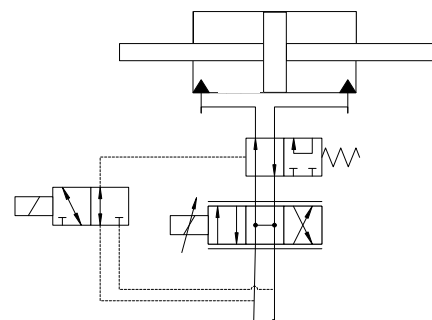


Fig. 1: Servo-hydraulic actuator scheme.

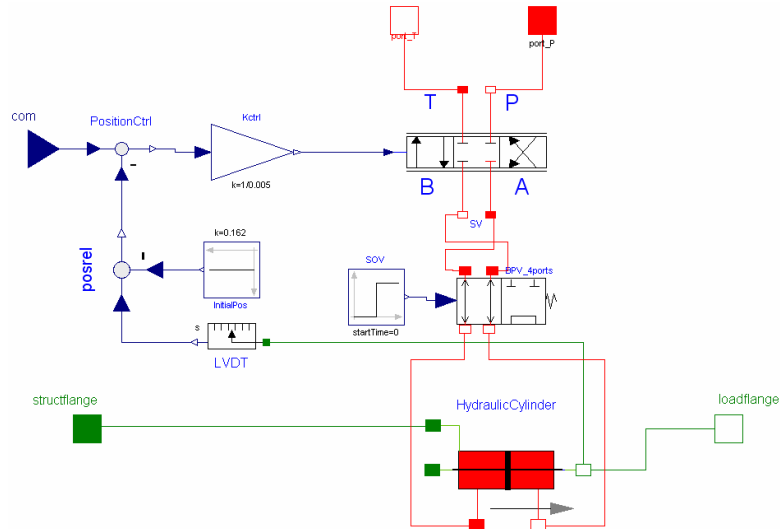


Fig. 2: Modelica-Dymola diagram of the servo-hydraulic actuator.

Hydraulic fluid	MIL-H-5606B
Supply pressure	210 bar
Return pressure	5 bar
Maximum internal leakage	< 1% no-load max flow rate
Servovalve bandwidth	> 60 Hz
Actuator friction force	< 5% stall force

Table 2 Additional requirements for SHA sizing.

The definition of the SHA functional parameters has been carried out with reference to the data given by Table 1, together with the additional requirements provided by Table 2.

The resulting object-model, entirely developed in the Modelica-Dymola environment, is reported in Fig. 2. The external interfaces of the component are the position command coming from the flight control computer, two hydraulic ports for the integration with the hydraulic plant, and two mechanical joints, for the connection with the structure of the aircraft and with the control surface respectively.

All the parts of the SHA model have been created using the basic components of the HyLib library of Dymola, except for the four-way bypass valve, which has been specifically created by the authors.

2.2 Electro-hydrostatic actuator

Figure 3 shows the working scheme of an electro-hydrostatic actuator (EHA).

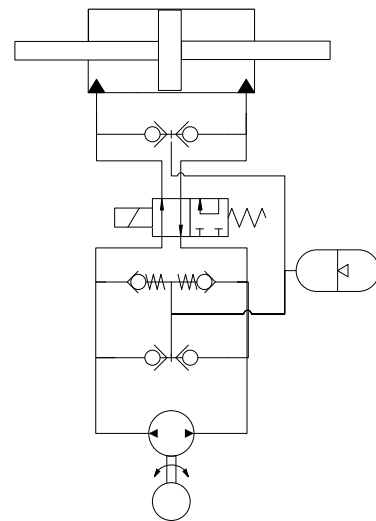


Fig. 3: Electro-hydrostatic actuator scheme.

The basic feature of this technological solution is the lacking of a centralised hydraulic plant for the actuator power supply. The hydraulic power regulation is here obtained by a small-size fixed-displacement pump, driven by a speed-controlled electrical motor¹. The EHA

¹ An alternative solution is given by the IAPTM actuation, in which a variable-displacement pump is driven by an electrical motor with fixed operating speed [8].

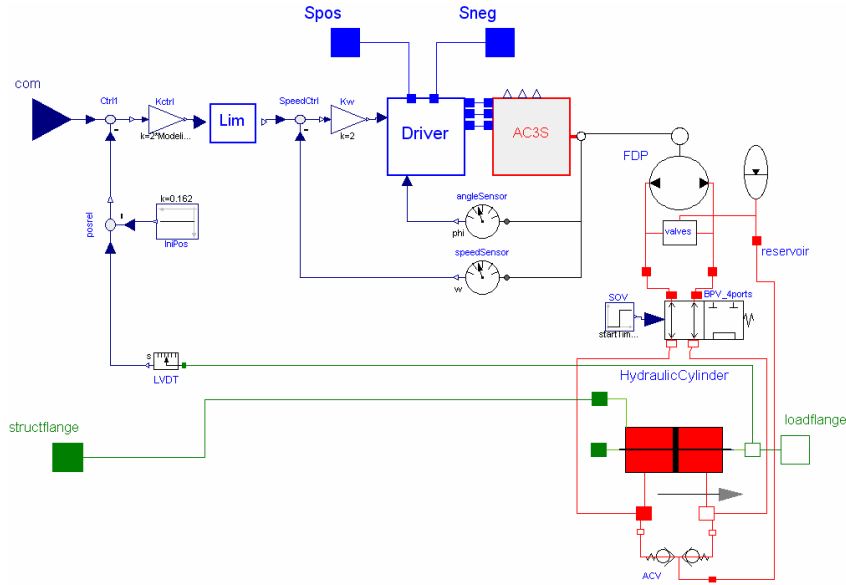


Fig. 4: Modelica-Dymola diagram of the of the electro-hydrostatic actuator.

assembly also includes a pressurised reservoir to avoid cavitation and to provide relief functions in case of over-loads. The actuator control system is more sophisticated with respect to the SHA solution, since three closed-loop controls are necessary, respectively on actuator position, motor speed, and motor current.

As discussed by many authors [2, 8], the EHA technology represented for years the most reliable and suitable solution for “more-electric” aircraft, where electrically-powered systems gradually reduce the use of centralised plants for pneumatic and hydraulic power generation, with the purpose of achieving eco-compatibility targets, maintenance cost reduction, more efficient power usage.

Hydraulic fluid	MIL-H-5606B
Maximum working pressure	210 bar
Reservoir pressure	10 bar
Reservoir capacity	< 1 litres
Maximum internal leakage	< 1% no-load max flow rate
Pump inertia	< 0.001 kg m ²
Motor type	3-phase AC synchronous
Motor inertia	< 0.001 kg m ²
Motor maximum current	< 40 A _{rms}
Motor speed response bandwidth	> 40 Hz
Current response bandwidth	> 400 Hz
Actuator friction force	< 5% stall force

Table 3 Additional requirements for EHA sizing.

The data given in Tables 1 and 3 have been used for sizing the EHA. The resulting Modelica-Dymola component is reported in Fig. 4. In this case, the external interfaces are the position command, two electrical pins for the electrical power supply (270 V_{DC}) and the two mechanical joints to the aircraft structure and to the control surface.

A significant effort has been made for developing this object-model, since the basic components provided by the Dymola libraries were not sufficient for the scopes. Actually, the miniaturised fixed-displacement pump (FDP) with integrated reservoir, the tri-phase AC current driver, and the brushless electrical motor have been specifically created during the work.

It must be mentioned that, in order to obtain practical results, the functional parameters of the tri-phase AC synchronous motor have been set by selecting an off-the-shelf electrical motor that demonstrated to be suitable for the application².

2.3 Electro-mechanical actuator

As depicted by Fig. 5, the electro-mechanical actuator (EMA) offers the simplest working scheme: the aerodynamic surface is

² Moog G415-4xx (nominal power: 3.4 kW; continuous stall torque: 12 Nm; peak torque: 26 Nm; nominal speed: 3500 rpm; current-torque gain: 1.1 Nm /A_{rms}).

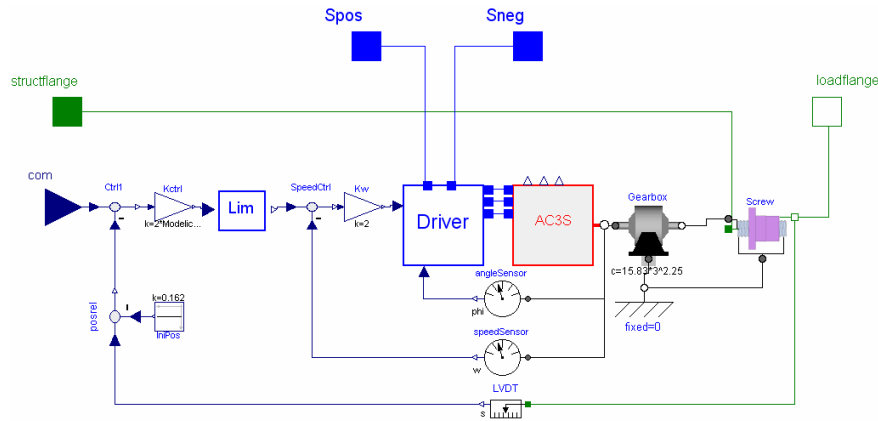


Fig. 6: Modelica-Dymola diagram of the electro-mechanical actuator.

moved by means of a screw jack, driven by a speed-controlled electrical motor.

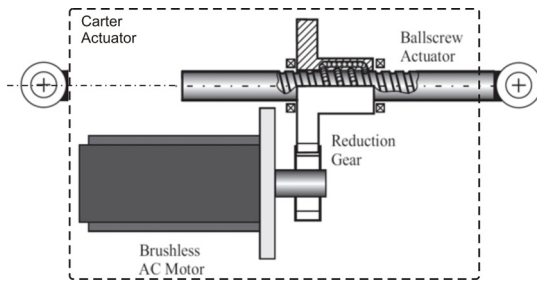


Fig. 5: Electro-mechanical actuator scheme.

The actuator control system is very similar to that of the electro-hydraulic actuator, with the implementation of actuator position, motor speed and motor current closed-loop controls.

This type of actuation is the most convenient in terms of eco-compatibility, cost reduction, and (as further pointed out by the simulation results) optimal power management. On the other hand, the main drawbacks are related to reliability and fail-safe operation [9]. Actually, the susceptibility to mechanical jam of the screw jack, the effects of the mechanical transmission free-play in case of flutter, as well as the more difficult implementation of “damping” devices in case of motor failure, still lead to consider the EMA technology as a future solution, especially for primary flight control applications.

Concerning the modelling activity, the actuator parameters have been defined with the data of Tables 1 and 4, while the Modelica-Dymola scheme of the EMA is reported in Fig. 6.

Motor type	3-phase AC synchronous
Motor inertia	$< 0.001 \text{ kg m}^2$
Motor maximum current	$< 40 \text{ A}_{\text{rms}}$
Motor speed response bandwidth	$> 40 \text{ Hz}$
Current response bandwidth	$> 400 \text{ Hz}$
Mechanical transmission type	Ball-screw jack
Actuator friction force	$< 5\% \text{ stall force}$

Table 4 Additional requirements for EMA sizing.

2.4 Performances of the isolated actuators

In order to verify the design requirements, preliminary simulation tests have been performed, by commanding the isolated actuators with a step command, while a spring-type load (0.6 kN/mm) is applied on the control surface joint.

Figures 7-8 report the simulation results obtained by step-driving the actuators of 5 mm far from the zero-load condition. It can be noted that all the actuators exhibit satisfactory performances in terms of position response, in both dynamic and static conditions, Fig. 7.

Concerning the power absorption aspects, Fig. 8 highlights that the SHA absorbs hydraulic power even in no-load conditions, as a result of the unavoidable fluid leakages through the pressure and the return ports of the servovalve. On the other hand, the EHA and the EMA exhibit a “power on-demand” behaviour, which is crucial for energy savings. During the transient motion, the EMA and the EHA require higher peak powers since the actuator motion directly depends on the motor shaft dynamics,

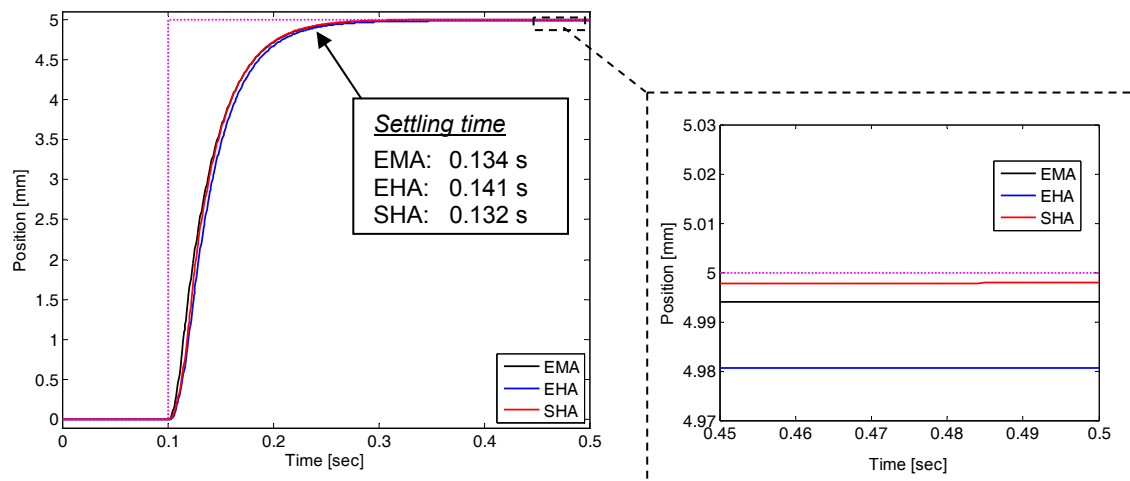


Fig. 7: Step response of the three actuators.

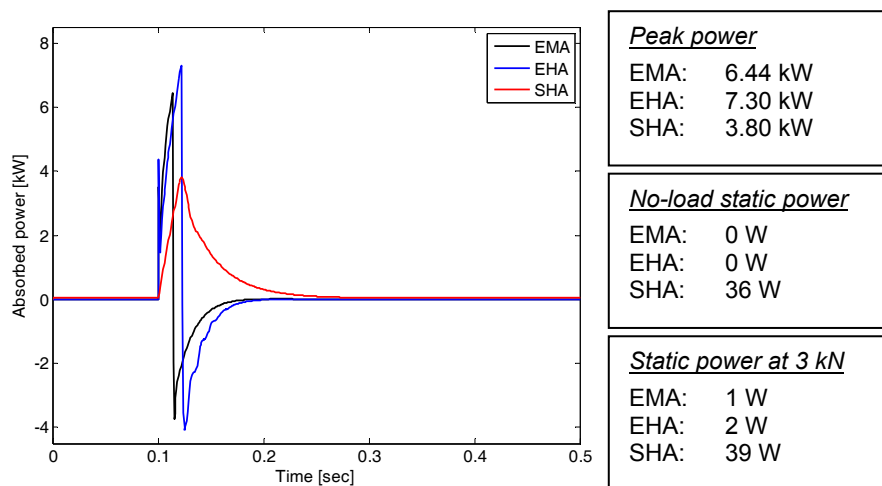


Fig. 8: Power absorption of the three actuators during the step response.

and adequate jack accelerations can be achieved only with high values of current (i.e. torque). On the other hand, the SHA peak power is lower, since the piston acceleration depends on the dynamics of fluid pressure in the hydraulic cylinder, which can be rapidly connected with the high/low pressure levels of the hydraulic plant. As a result, a small amount of flow rate absorption is sufficient to rapidly vary the pressure levels in the cylinder, thus obtaining the necessary acceleration.

These considerations will be deepened and detailed in the section 4, where the power absorption at system level will be addressed.

3 Actuation system models

To obtain practical results for aircraft applications, the model of an entire flight control actuation system has been created, simulating the mechanical, structural, and aerodynamic interfaces of the actuators.

3.1 Mechanical/structural interface

For each of the five flight control surfaces, a model of the actuator mechanical interface has been created, by reproducing an oscillating-arm kinematics, in which the surface deflection implies both a rotation of the actuator case

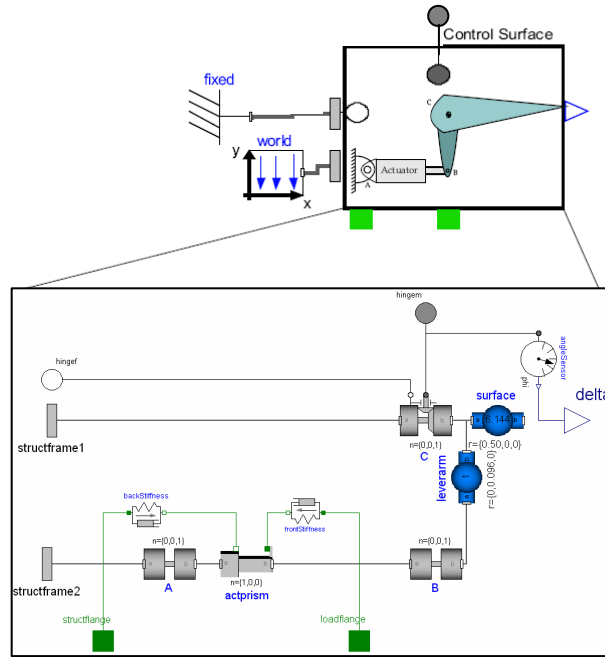


Fig. 9: Modelica-Dymola diagram of the mechanical/structural interface of the actuators.

and a translation of the actuator jack with respect to the case itself, Fig. 9.

To account for the elasticity of the actuator links (Table 1), the model also includes the use of two spring-damper components of the Modelica.Mechanics.Translational library, Fig. 9.

3.2 Hinge moment model

The aircraft actuation system model also includes the simulation of control hinge moments. According to the definition given in [13], the aerodynamic hinge moment on a generic control surface is given by Eq. 1:

$$H_c = \frac{\rho U_c^2}{2} mac_c^2 s_c C_{Hc}(M, \alpha_c, \delta_c) \quad (1)$$

where ρ is the air density, U_c is the local airspeed, mac_c is the mean aerodynamic chord of the control surface considered as an isolated wing, s_c is the span of the flapped portion of the reference aerodynamic surface (wing, horizontal tail, rudder) and C_{Hc} is the hinge moment coefficient. The last coefficient is a function of the Mach number, of the aerodynamic surface

angle-of-attack (α_c), and of the control surface deflection (δ_c).

The hinge moment coefficient is generally a nonlinear function of angle-of-attack and control deflection, but, at small incidences, a linear approximation is typically used for preliminary design, obtaining predictions on hinge moment coefficient derivatives with an accuracy of about 10% [13, 14], Eq. 2.

$$C_{Hc} = C_{Hc0} + b_{1c} \alpha_c + b_{2c} \delta_c \quad (2)$$

The linearity of hinge moment coefficient with respect to angle-of-attack and control deflection is valid only in a limited range. The extension of this range depends on the wing section, on control geometry, as well as on the conditions of the airflow, so that a generalized prediction is not possible. Though no systematic quantitative data can be given for the post-linear behaviour, the linear range of the hinge moment coefficient can be considered similar to that of the lift coefficient ($\pm 10^\circ$). Outside the linear range, the flow typically separates over the control surface, and hinge moments increase more rapidly [13].

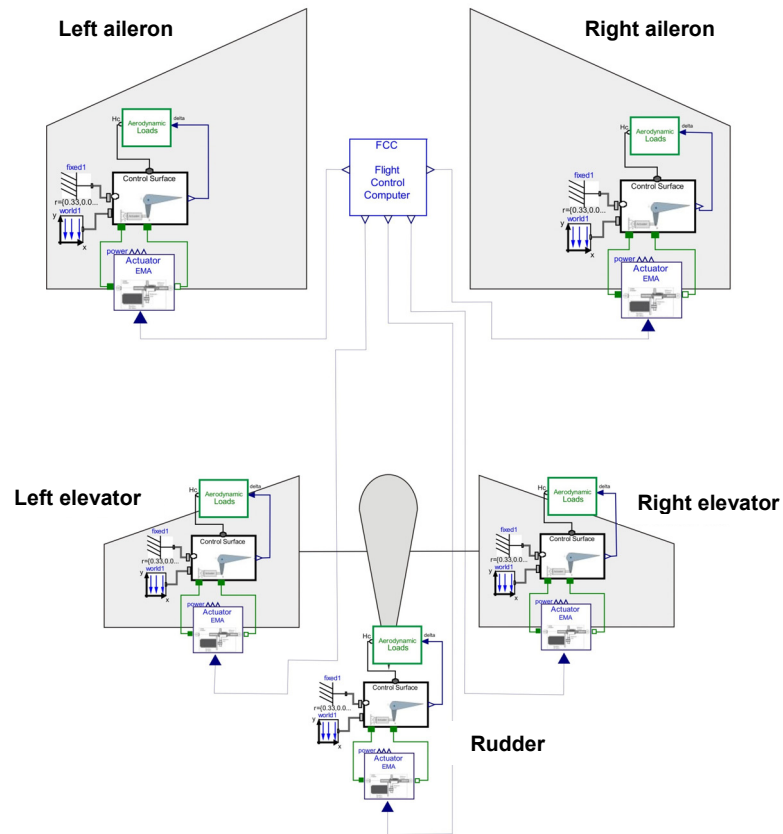


Fig. 11: Modelica-Dymola diagram of the primary flight control actuation system.

The hinge moment evaluation in the post-linear range can be important for the actuation system design, but, for the purposes of this work, it has been roughly modelled as reported in Fig. 10, by saturating it at the maximum value obtained in the linear range.

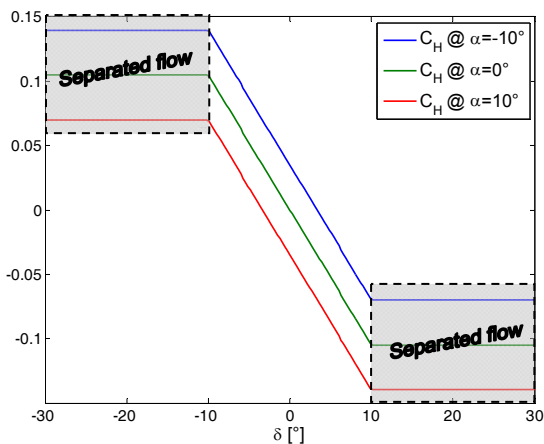


Fig. 10: Hinge moment coefficient for the elevator.

3.3 Complete system model

The study has been referred to a basic primary flight control system with two ailerons, two elevators and one rudder. Figure 11 shows the resulting Modelica-Dymola diagram of the entire actuation system.

4 Power absorption assessment

4.1 Reference flight conditions and sample flight manoeuvre

The power absorptions of the EMA, EHA and SHA systems have been assessed with reference to the same time history of the commands for the primary flight control actuators, as obtained by the flight simulator of a light military trainer aircraft.

Starting from an initial condition of horizontal trim flight (Table 5), the aircraft is

OBJECT-ORIENTED MODELLING OF FLIGHT CONTROL ACTUATION SYSTEMS FOR POWER ABSORPTION ASSESSMENT

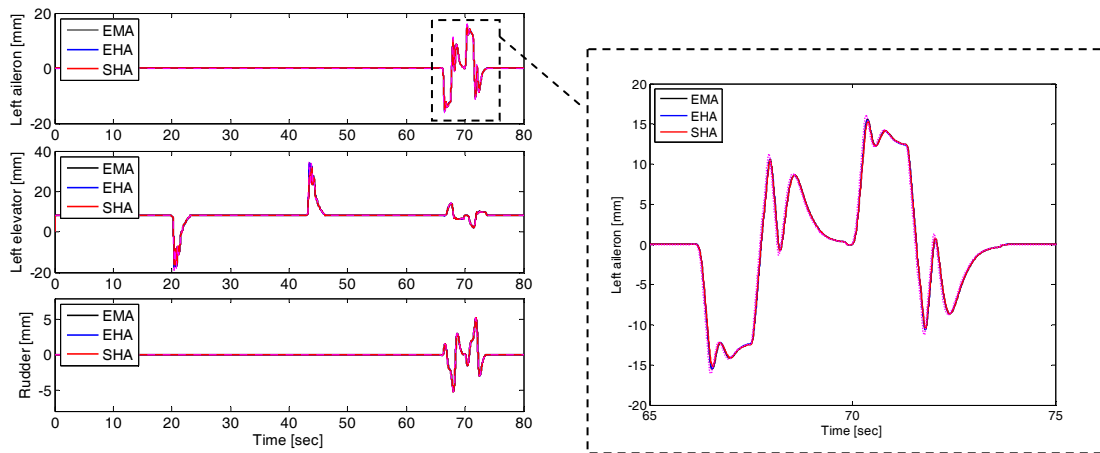


Fig. 12: Position response of the actuation systems during the flight manoeuvre.

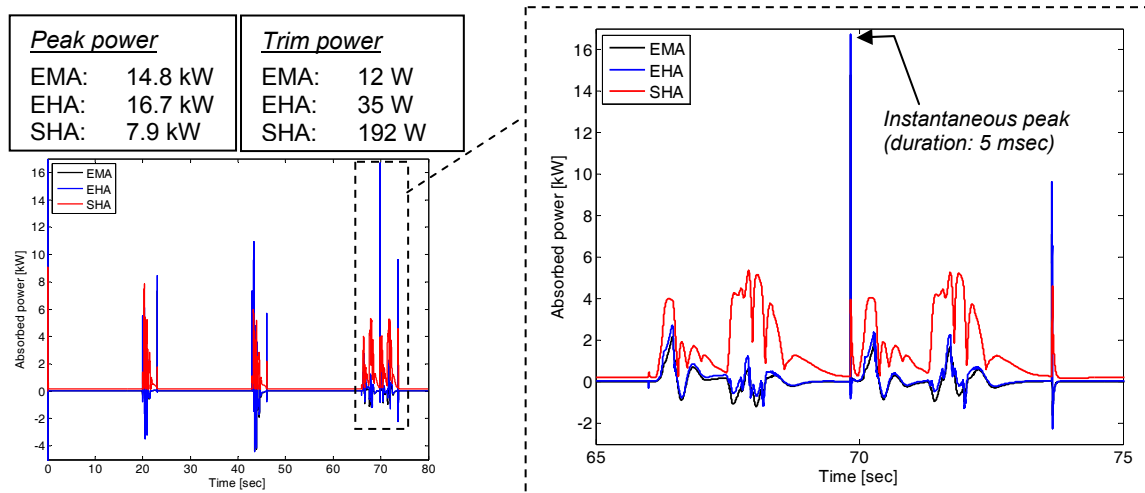


Fig. 13: Instantaneous power absorption of the actuation systems during the flight manoeuvre.

supposed to experience the following manoeuvre sequence:

- pull-up (at $t = 20$ sec);
- pull-down (at $t = 40$ sec);
- turning (at $t = 65$ sec).

Altitude	1000 m
Mach number	0.6
Aircraft angle-of-attack	-1.83°
Elevator deflection	4.89°

Table 5 - Initial flight conditions (horizontal trim).

Figure 12 reports the command time history for the flight control actuators, and it can be seen that all the actuation technologies generally provide a satisfactory tracking of the command signals.

4.2 System power absorption

The power absorptions of the three actuation systems are reported in Fig. 13. As a consequence of the discussion on the isolated actuators, the peak power of the SHA system is less than that required by the other plants. However, for electrically-powered systems, the peak power calculated on the instantaneous absorption is not practical for power analysis purposes. As suggested in [12], an “averaged” power calculated on a time interval relevant for control electronics would be more significant, so the effective peak power requirements for EMA and EHA systems would be reduced.

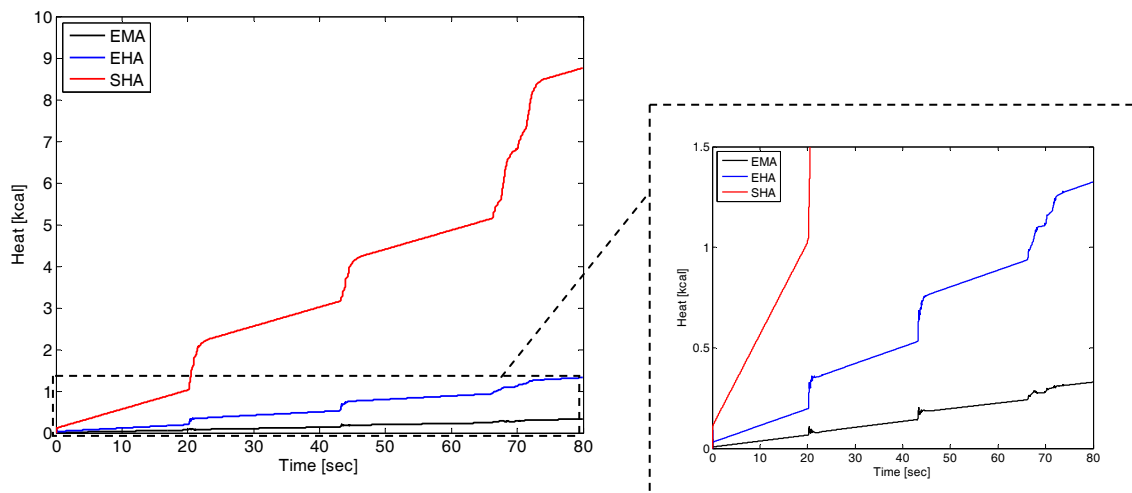


Fig. 14: Heat generated by the actuation systems during the flight manoeuvre.

Concerning the power absorption in static conditions (trim and successive static phases), the results confirm the superiority of the EMA technology in terms of energy savings. For holding the flight actuators at fixed deflections, the EMA system absorbs only 12 W, the EHA plant 35 W (due to the internal leakages of the miniaturised pump), while the traditional SHA system consumes up to 192 W.

Nevertheless, it is also important to evaluate the predictions on the heat generated by the actuation systems, Fig. 14. The SHA system, being less efficient, generates a huge amount of heat, but this heat is transported by the hydraulic fluid far from the actuator, up to the hydraulic plant reservoir where dedicated heat exchangers provide refrigeration. On the other hand, the heat generated by EMA and EHA is very low, but also strongly localised, thus implying a rapid increase of the actuator operating temperature if heat dissipation is not efficient.

Conclusion

The power absorption of three aircraft actuation systems characterised by different technologies (SHA, EHA and EMA) has been assessed via object-oriented modelling. Simulation results point out that the three solutions provide similar results from a position response point of view, and confirm the superiority of the EMA solution in terms of

energy savings, thanks to a minimum level of absorbed power in static conditions. For holding the flight actuators at fixed deflections, the EMA power absorption is about three times less than the EHA system, and about sixteen times less than the SHA plant. Nevertheless, the predictions on the heat generated by the actuation systems arose important thermal issues. The huge amount of heat generated by a SHA system is not problematic for the actuator functionality, since it is transported by the fluid up to the hydraulic plant reservoir, where dedicated heat exchangers provide refrigeration. In the case of EMA and EHA, the generated heat is very low, but also strongly localised, thus implying a rapid increase of the actuator operating temperature if heat dissipation is not efficient.

References

- [1] Emadi A., Ehsani M. Aircraft power systems: technology, state of the art, and future trends. *IEEE AES Systems Magazine*, January 2000, pp. 28-32.
- [2] Cutts S. J.. A collaborative approach to the more electric aircraft. Proceedings of the IEE Conference on Power Electronics, Machines and Drives, Bath (UK), pp. 223-228, 2002.
- [3] Howse M.. All electric aircraft. *IEE Power Engineering Journal*, Vol. 17, No. 4, pp. 35-37, 2003.
- [4] Rosero J. A., Ortega J. A., Aldabas E., Romeral L.. Moving towards a more electric aircraft. *IEEE A&E Systems Magazine*, March 2007, pp. 3-9.

- [5] Maldonado M. A., Korba G. J.. Power management and distribution system for a more electric aircraft (MADMEL) - Program status. *IEEE AES Systems Magazine*, December 1999, pp. 3-8.
- [6] Schallert C., Pfeiffer A., Bals J.. Generator power optimisation for a more electric aircraft by use of a virtual iron bird. *Proceeding of the 25th International Congress of Aeronautical Sciences (ICAS)*, Hamburg (Germany), 2006.
- [7] Anastasio V., Di Donna L.. Power by wire meets environmental friendly requirements. *Proceedings of the XIX AIDAA National Congress*, Forli (Italy), 2007.
- [8] Botten S. L., Whitley C. R., King A. D.. Flight control actuation technology for next generation all-electric aircraft. *Technology Review Journal*, pp. 55-68, 2000.
- [9] Garcia A., Cusidò I., Rosero J. A., Ortega J. A., Romeral L.. Reliable electro-mechanical actuators in aircraft. *IEEE A&E Systems Magazine*, August 2008, pp. 19-25.
- [10] Elmqvist H., Mattsson S. E., Otter M.. Modelica – The new object-oriented modeling language. *Proceedings of the 12th European Simulation Multiconference (ESM'98)*, Manchester (UK), pp. 1-5, 1998.
- [11] Otter M., Elmqvist H.. Modelica: language, libraries, tools, workshop and EU-project RealSim, *Simulation News Europe*, pp. 3-8, 2000.
- [12] Bals J., Hofer G., Pfeiffer A., Schallert C.. Object-oriented inverse modelling of multi-domain aircraft equipment systems with Modelica. *Proceedings of the 3rd International Modelica Conference*, Linköping (Sweden), pp. 377-383, 2003.
- [13] ESDU Doc. No. 70011, 72024, 89009, 89010, 97020, C.01.01.01, C.01.01.03, C.01.01.04, C.04.01.00, C.04.01.01, C.04.01.02, C.04.01.03, C.04.01.04, C.04.01.06, C.04.01.08, F.05.01.01, Educational Science Data Unit Ltd, London (UK).
- [14] Hoerner S. F., Borst H. V.. *Fluid-dynamic lift: practical information on aerodynamic and hydrodynamic lift*. Borst-Hoerner, 1975.

Copyright Statement

The authors confirm that they, and/or their company or organization, hold copyright on all of the original material included in this paper. The authors also confirm that they have obtained permission, from the copyright holder of any third party material included in this paper, to publish it as part of their paper. The authors confirm that they give permission, or have obtained permission from the copyright holder of this paper, for the publication and distribution of this paper as part of the ICAS2010 proceedings or as individual off-prints from the proceedings.